BMC Developmental Biology

BioMed Central

Research article

The functional genomic response of developing embryonic submandibular glands to NF-kappaB inhibition

Michael Melnick*, Haiming Chen, Yan Min Zhou and Tina Jaskoll

Address: Laboratory for Developmental Genetics, University of Southern California Los Angeles, CA, USA

E-mail: Michael Melnick* - mmelnick@hsc.usc.edu; Haiming Chen - haimingc@hsc.usc.edu; Yan Min Zhou - zhou@hsc.usc.edu; Tina Jaskoll - tjaskoll@hsc.usc.edu

*Corresponding author

Published: 25 October 2001

BMC Developmental Biology 2001, 1:15

Received: 3 July 2001
Accepted: 25 October 2001

This article is available from: http://www.biomedcentral.com/1471-213X/1/15

Abstract

Background: The proper balance between epithelial cell proliferation, quiescence, and apoptosis during development is mediated by the specific temporal and spatial appearance of transcription factors, growth factors, cytokines, caspases, etc. Since our prior studies suggest the importance of transcription factor NF-κB during embryonic submandibular salivary gland (SMG) development, we attempted to delineate the emergent dynamics of a cognate signaling network by studying the molecular patterns and phenotypic outcomes of interrupted NF-κB signaling in embryonic SMG explants.

Results: SN50-mediated inhibition of NF-κB nuclear translocation in E15 SMG explants cultured for 2 days results in a highly significant increase in apoptosis and decrease in cell proliferation. Probabilistic Neural Network (PNN) analyses of transcriptomic and proteomic assays identify specific transcripts and proteins with altered expression that best discriminate control from SN50-treated SMGs. These include PCNA, GR, BMP1, BMP3b, Chk1, Caspase 6, E2F1, c-Raf, ERK1/2 and JNK-1, as well as several others of lesser importance. Increased expression of signaling pathway components is not necessarily probative of pathway activity; however, as confirmation we found a significant increase in *activated* (phosphorylated/cleaved) ERK 1/2, Caspase 3, and PARP in SN50-treated explants. This increased activity of proapoptotic (caspase3/PARP) and compensatory antiapoptotic (ERK1/2) pathways is consistent with the dramatic cell death seen in SN50-treated SMGs.

Conclusions: Our morphological and functional genomic analyses indicate that the primary and secondary effects of NF-κB-mediated transcription are critical to embryonic SMG developmental homeostasis. Relative to understanding complex genetic networks and organogenesis, our results illustrate the importance of evaluating the gene, protein, and activated protein expression of multiple components from multiple pathways within broad functional categories.

Background

Following a classic epithelial-mesenchymal interaction developmental program, the mouse neonatal submandibular salivary gland (SMG) is comprised of large and small ducts which terminate in lumen-containing, presumptive acini that express embryonic mucin [1–8].

Progressive prenatal morphogenesis begins as a solid outgrowth from the oral epithelium around E11.5, and is best conceptualized in stages [9]: *Initial Bud, Pseudoglandular, Canalicular,* and *Terminal Bud*. Epithelial cell proliferation is found in all stages, even after well-defined lumen formation in the *Terminal Bud* Stage. Epithelial cell apoptosis begins with the onset of lumen formation in the *Canalicular* Stage.

The proper balance between SMG epithelial cell proliferation, quiescence, and apoptosis is mediated by the appearance of transcription factors, growth factors, cytokines, caspases, etc. at specific times and places [10–14]. These SMG cellular and extracellular components may be visualized as a *Connections Map* which details the functional relationships within and between pathways (Fig. 1).

Complex networks of biological signaling pathways (Fig. 1) emerge from the interconnections of simple pathways under local control [15–17]. As such, these cellular pathways are more analogous to the mostly redundant, overlapping neural network of the brain than to traffic grids of intersecting streets and interacting vehicles. There are two general, not mutually exclusive, classes of interconnections: (1) junctions which serve as signal integrators and (2) nodes which split the signal and route them to multiple outputs [18]. Understanding the nonlinear dynamics of these interconnections is intrinsic to understanding the regulation of SMG morphogenesis. This requires the integration of transcriptomic, proteomic, phenomic, and bioinformatic approaches, not least because development, in its most basic sense, is genes plus context [19–22].

With the present experiments, we sought a glimpse of the extraordinarily complex behaviors of a focused signaling network (Fig. 1). To this end, we studied the molecular patterns and phenotypic outcomes of a nodal "short circuit", i.e., the inhibition of NF-κB activation and translocation to the nucleus to bind to NF-κB response genes. In most cell types, the NF-κB p50/p65 heterodimer is maintained as an inactive form in the cytoplasm bound to the inhibitory protein IκB. Exposure of cells to stimuli of NF-κB induces the rapid phosphorylation and subsequent degradation of IκB proteins. Released NF-κB dimers then translocate to the nucleus, bind to its cognate DNA elements, and induce the expression of target genes [23–25]. Activated, nuclear translocated, NF-κB transcription factor has been documented in the mouse embryo from the 1-cell stage onward [26,27]. Activated NF-κB translocation into the nucleus, directly or indirectly, effects the transcriptional control of over 150 target genes [28]. NF-κB enhances cell proliferation by stimulating the expression of cytokines such as TNF, IL-1, IL-2, IL-6, and IL-8, among others [28,29]; NF-κB inhibits apoptosis by inducing TRAF and clAP expression which suppresses Caspase 8 activation [30], and by inhibition of p53 transactivation [31,32].

We interrupted the NF-κB signal in embryonic SMG explants using the cell-permeable peptide SN50, a potent inhibitor of NF-κB nuclear translocation [25,26], [33–35]. SN50-mediated inhibition of NF-κB nuclear translocation in SMG explants results in extensive apoptosis and a very substantial decline in cell proliferation. Functional genomic analyses demonstrate that inhibition of NF-κB signaling is associated with the altered expression of numerous components of the genetic network of related signaling pathways. This modified expression of genes and proteins associated with the inhibition of the cell cycle and the induction of apoptosis, as well as the increased activation of proapoptotic and compensatory antiapoptotic pathways, provides a "snapshot" of the broad primary and secondary effects of NF-κB signaling during SMG development.

Results and discussion

NF-κB is well visualized in embryonic SMGs. In the *Pseudoglandular* Stage (~E14), NF-κB is primarily immunodetected in SMG branching epithelia, and, to a much lesser extent, in the mesenchyme (Fig. 2A). At the *Canalicular* Stage (~E15–16), NF-κB is primarily immunolocalized in the central regions of the terminal buds, and to a lesser extent, in the ductal cells facing the lumina (Fig. 2B, double arrows). By the *Terminal Bud* Stage (~E17–19), NF-κB is diffusely distributed throughout ductal and terminal bud epithelia (Fig. 2B, double arrowheads), with the intensity of immunostain being markedly diminished compared to the *Canalicular* Stage.

NF-κB inhibition and SMG phenotype

E15 SMG primordia were cultured for 2 days in the presence or absence of the cell-permeable peptide SN50, a potent inhibitor of NF-κB nuclear translocation [33–35]. SN50 is composed of a nuclear localization sequence (NLS) for NF-κB p50 linked to a cell-permeable carrier [33–35]. SN50 blocks the intracellular recognition mechanism for the NLS on NF-κB, thus inhibiting NF-κB's translocation through the nuclear pore. After 2 days in culture, SN50-treated explants exhibit a substantial decrease in gland size and branching morphogenesis compared to controls (compare Fig. 3A to 3B). These 2-day SN50-treated explants demonstrate a highly significant 81% decline ($t_4 = 26.25$; $p < 0.001$) in cell proliferation (Fig. 3A, B; Fig. 4A) and a significant 10-fold increase ($t_4 = 7.98$; $p < 0.001$) in apoptosis (Fig. 3C, D; Fig. 4B). This substantial increase in apoptosis is associated with a highly significant > 4-fold increase ($t_4 = 22.66$; $p < 0.001$) in *activated* (phosphorylated) p53

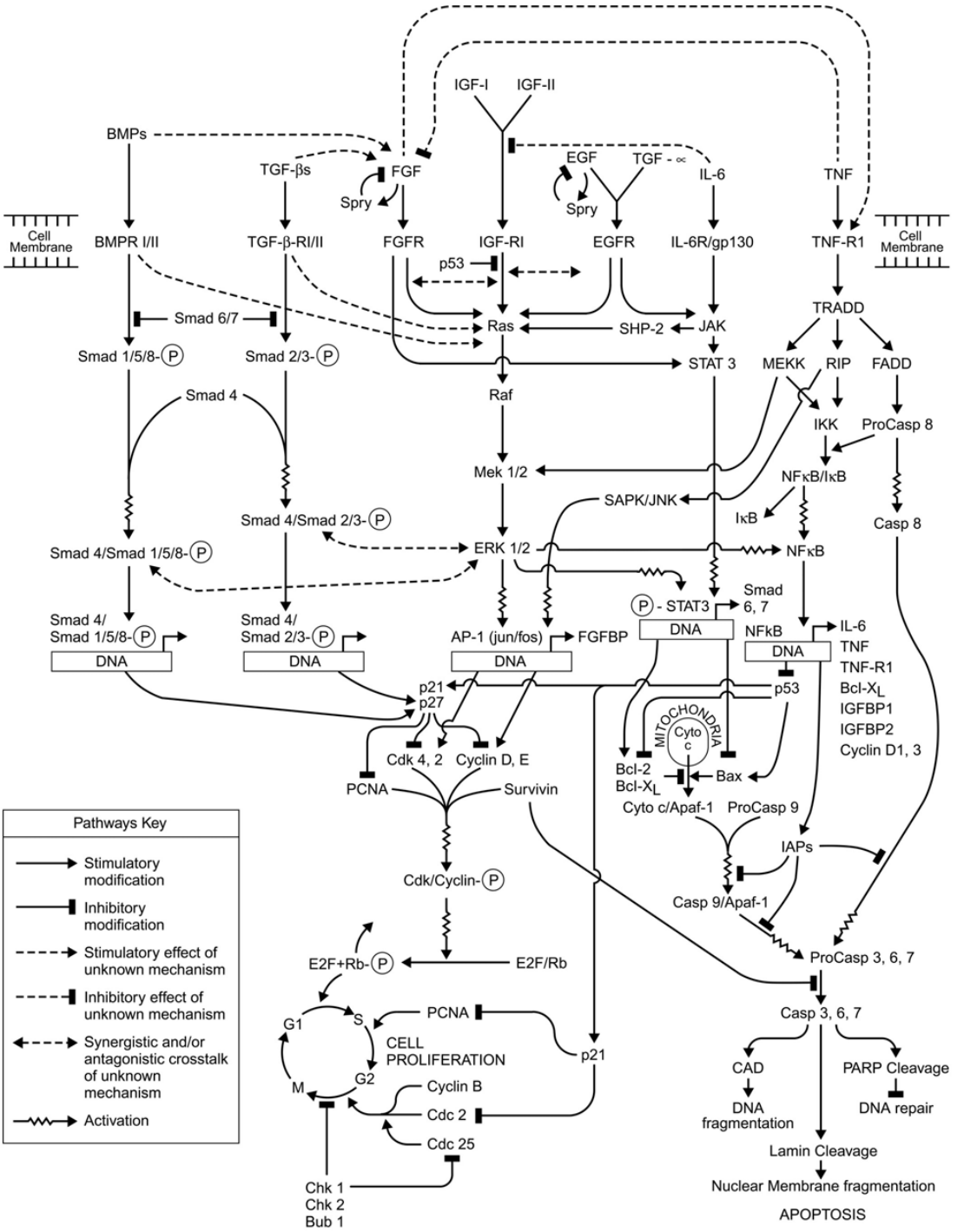

Figure 1

Connections Map. This signaling map reflects the pathways investigated in SMGs. Known and putative connections are based on references [6], [11], [23], [36], [76]-[108].

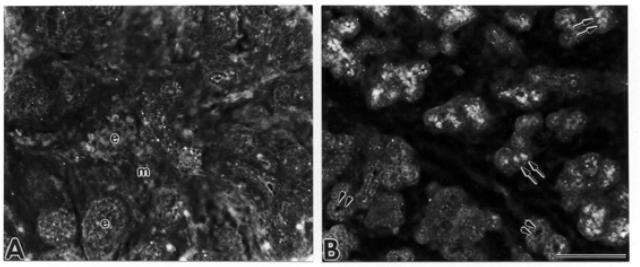

Figure 2
NF-κB immunolocalization during embryonic SMG development. A. *Pseudoglandular* Stage. B. *Canalicular* and *Terminal Bud* Stages. During embryonic mouse SMG development, the SMG primordium branches by repeated furcation at the distal ends of successive buds to produce a bush-like structure comprised of a network of elongated epithelial branches and terminal epithelial buds surrounded by loosely packed mesenchyme in the *Pseudoglandular* Stage. We evaluated the spatial distribution of NF-κB (p65) protein in the *Pseudoglandular* Stage (A) and demonstrated that NF-κB is diffusely distributed throughout the branching epithelia, and to a lesser degree, in the mesenchyme. As development continues, the SMG epithelia branches and buds hollow out by epithelial cell apoptosis during the *Canalicular* and *Terminal Bud* Stages to form the ductal system and presumptive acini. Because the embryonic SMG develops by repeated epithelial end bud branching, the morphogenetic state of terminal bud clusters differs between SMG regions, dependent on the time of branch formation. Thus both the *Canalicular* (double arrows) and the *Terminal Bud* (double arrowheads) Stages can be seen in B. In the *Canalicular* Stage (B, double arrows), NF-κB p65 is primarily immunodetected in the central region of the terminal buds. By contrast, NF-κB p65 is diffusely distributed in *Early Terminal Bud* Stage (B, double arrowheads) epithelia in terminal buds which exhibit lumina. Similar localization patterns were immunodetected for NF-κB p50 protein (not shown). Bar: 50 μm.

(Fig. 5). This result is not surprising, given that NF-κB inactivates p53 [32].

To demonstrate that this SN50 phenotype is consequent to SN50-mediated inhibition of NF-κB nuclear translocation and not the nonspecific effect of exogenous peptide, we compared E15 + 2 SMG phenotypes in explants cultured in control media, 100 μg/ml SN50 peptide, or 100 μg/ml mutant SN50 (mSN50) peptide. As expected, we found a marked difference between control and SN50-treated SMGs but none between control and mutant peptide-treated explants (data not shown). In addition, since TNF/TNFR1 signaling has been shown to induce embryonic SMG cell proliferation and inhibit apoptosis *in vitro* [13] and TNF/TNFR1 signal transduction primarily signals by induction of NF-κB nuclear translocation [36], we postulated that TNF supplementation should have no inductive effect on SN50-treated SMGs.

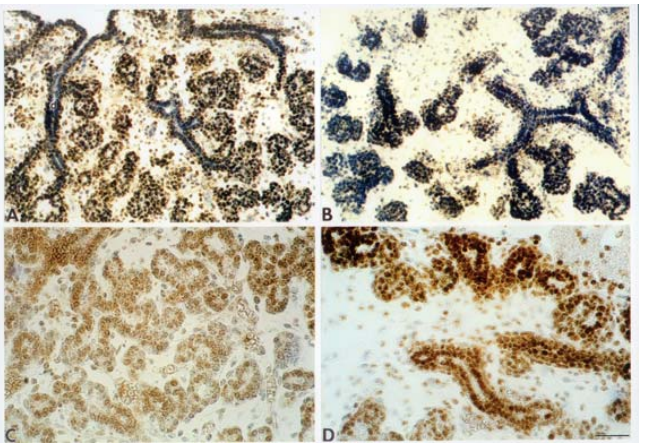

Figure 3
Cell proliferation and apoptosis. E15 SMG primordia were cultured in the presence or absence of 100 μg/ml SN50 peptide for 2 days (E15 + 2) and cell proliferation and apoptosis was determined. A., B. Cell proliferation. There is a marked decrease in cell proliferation (PCNA positive/brown color) with SN50 treatment (B) compared to control (A). Note that these sections were counterstained in hematoxylin; thus the cytoplasm in non PCNA-positive cells appears blue. C., D. Apoptosis. SN50 treatment (D) induced a notable increase in apoptotic positive nuclei (dark brown color) in ductal and terminal bud epithelia compared to control (C). Note that since these sections were not counterstained; thus the cytoplasm appears light brown. Bar: 50 μm.

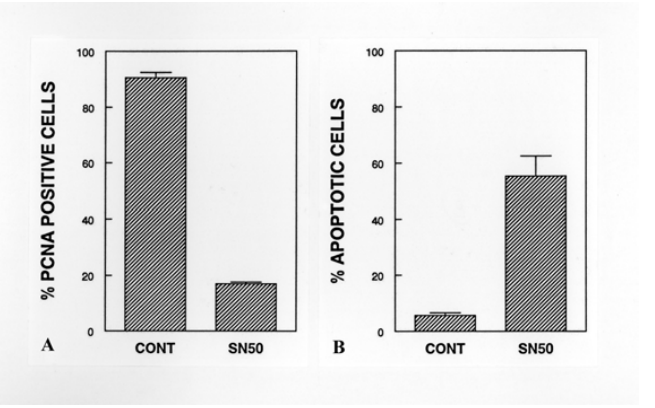

Figure 4
Quantitation of cell proliferation and apoptosis in control and SN50-treated E15 + 2 SMG explants. The data presented here is the results of 3 independent samples. Mean ± SEM percent positive epithelium: each bar is the mean of 3 independent samples, each sample representing counts in 3 randomly selected regions of that sample; percents were arcsin transformed for analysis. A. SN50-treated SMG explants have an 81% decline in cell proliferation. B. SN50-treated SMG explants have a 10-fold increase in apoptosis.

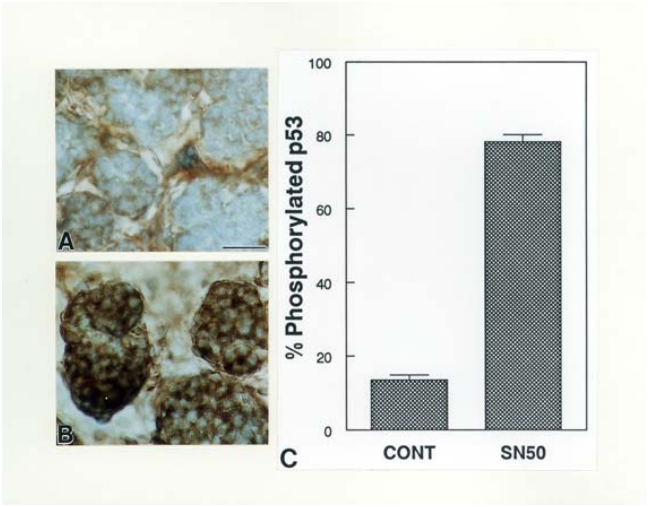

Figure 5
SN50 treatment induces a significant increase in *activated* (phosphorylated) p53. We detect a notable increase in *activated* p53 (brown color) in E15 + 2 SN50-treated (100 μg/ml) explants (B) compared to control (A). Bar: 50 μm. C. Quantitation of *activated* p53 in control (CONT) and SN50-treated E15 + 2 explants. The data presented here represents 3 independent samples. Mean ± SEM percent positive epithelium: each bar is the mean of 3 independent samples, each sample representing counts in 3 randomly selected regions of that sample; percents were arcsin transformed for analysis. A highly significant greater than 4-fold increase in *activated* p53 is seen between control and SN50-treated explants.

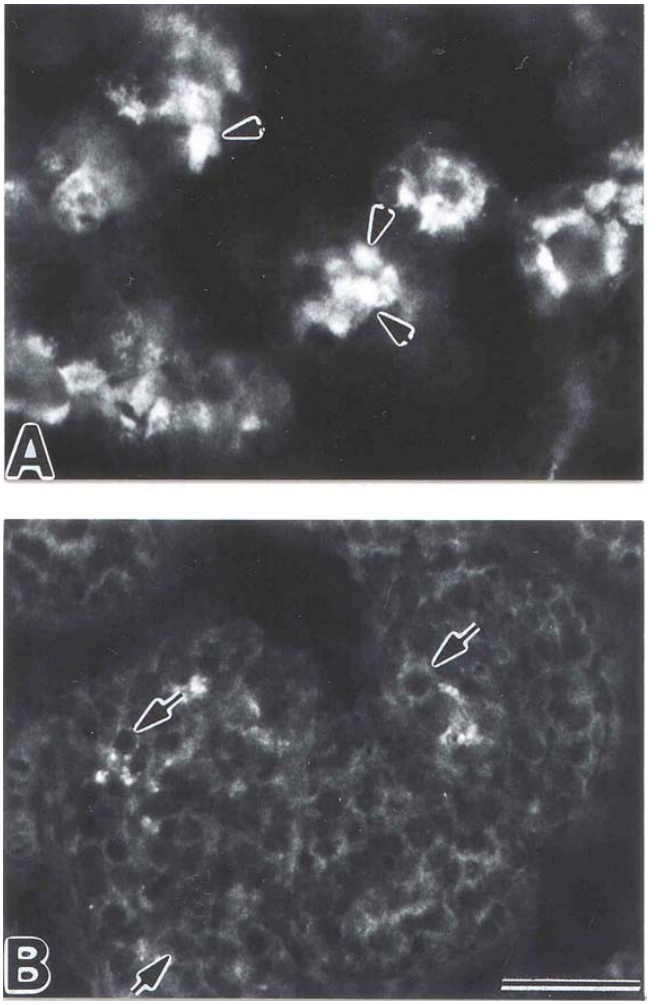

Figure 6
TNF-induced NF-κB nuclear translocation is inhibited by SN50 treatment. We evaluated the pattern of NF-κB p65 distribution in E15 SMG primordia cultured for 7 days in 10 U/ml rTNF (A) or 100 μg/ml SN50 + 10 U/ml rTNF (B) supplementation. In TNF-supplemented explants (A), NF-κB is detected in SMG terminal bud cell nuclei (arrow heads). By contrast, NF-κB is absent from cell nuclei (arrows) in TNF + SN50-supplemented explants (B). Rather, a weak, diffuse pattern of NF-κB immunolocalization in the cytoplasm is seen. Similar results were observed for NF-κB p50 immunolocalization (not shown). Bar, 100 μm.

Thus, we cultured E15 control, SN50-treated, and mSN50-treated explants in the presence of TNF (rTNF, 10 U/ml) supplementation for 4 or more days. In this set of experiments, we extended the culture period to provide sufficient time to allow for possible TNF-mediated recovery. TNF supplementation induced NF-κB (p50 and p65) translocation (Fig. 6A), a marked increase in explant size, and a notable increase in cell proliferation (not shown); similar results were seen in TNF+ mSN50-treated explants (not shown). By contrast, NF-κB redistribution was not found in explants cultured in TNF + SN50 (Fig. 6B); rather, NF-κB was absent from epithelial cell nuclei and exhibited a very weak, diffuse cytoplasmic distribution. Moreover, TNF supplementation was unable to rescue the abnormal SN50 phenotype. Finally, the identical response of control and mSN50-treated SMG explants to TNF supplementation provides further evidence that this mutant peptide had no effect on NF-κB activation.

Transcriptomic analysis

To investigate transcriptional responses to NF-κB inhibition, we analyzed control and SN50-treated E15 + 2 SMG explants using cDNA arrays. Of the 1176 transcripts assayed on these arrays (including transcription factors, cell cycle regulators, growth factors, etc.), 691 (~60%) demonstrated a 1.5-fold or greater increase or decrease in expression with SN50-induced NF-κB inhibition (Fig. 7). Of these, we focused our attention on those signal transduction, cell cycle, and apoptosis transcripts related to the *Connections Map* (Fig. 1). With inhibition of NF-κB translocation into the nucleus, 53 *Connections Map*

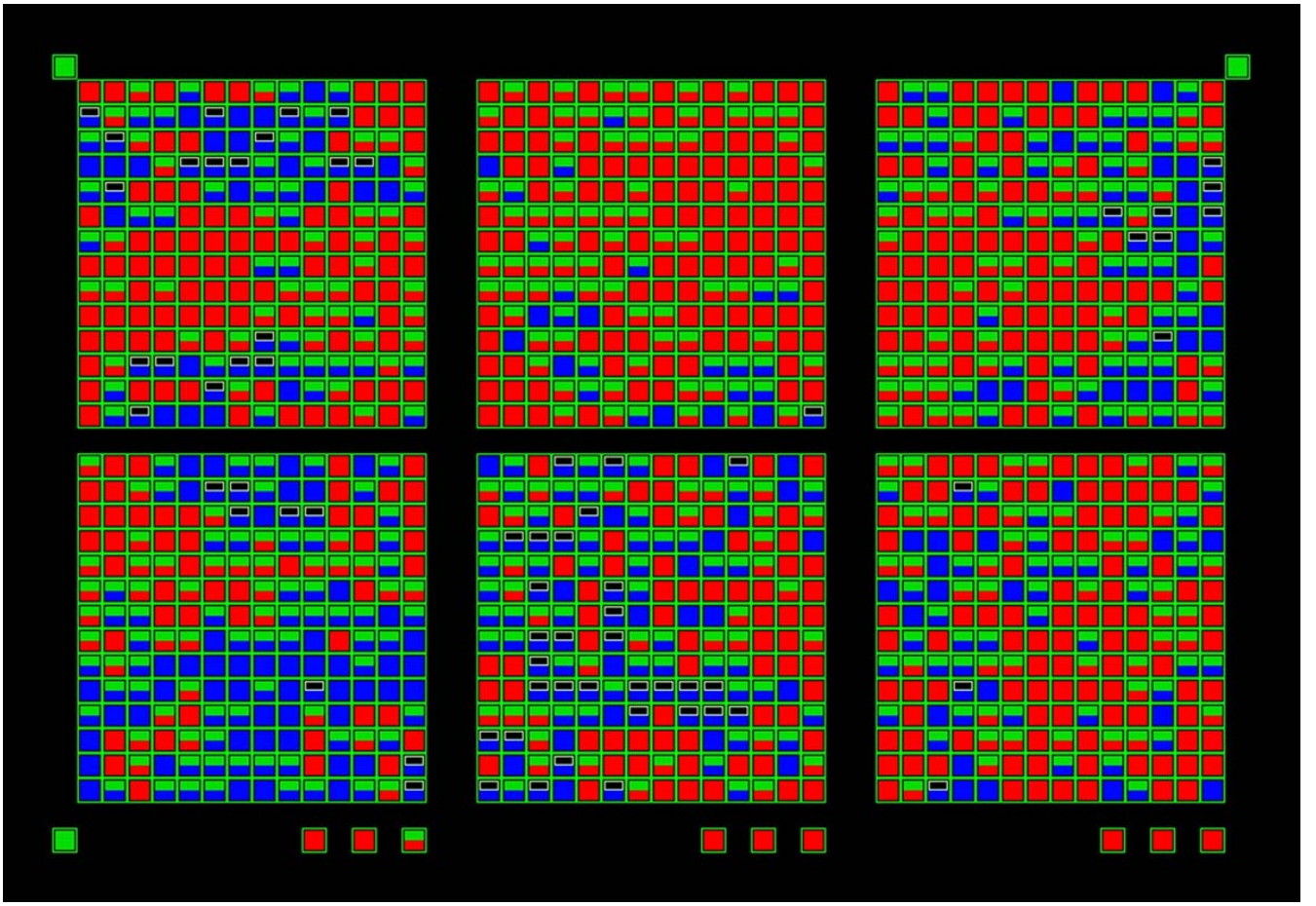

Figure 7
Comparison view of composite cDNA Expression Arrays. We analyzed differences in the relative abundance of transcript levels in control and 100 μg/ml SN50-treated E15 + 2 explants. This composite represents the changes in 3 independent experiments. It consists an array of boxes, each of which represents a specific gene. For a complete list of the genes and their position on this Expression Array, as well as the GenBank accession numbers, please see [atlas.clontech.com] . The color of each half-box reflects the calculated values for Gene Expression Ratio (top) and Gene Expression Differences (bottom): Red = upregulation; Blue = downregulation; Green = equal expression; Black = background level. Comparison is made between two composite arrays, each of which is a mean of 3 independent arrays. The signals of the composite SN50-treated SMG array is analyzed with respect to the composite control SMG array. In this comparison view, boxes which are black in the upper half indicate an "undefined" ratio because the signal for the SN50-treated SMG array is at the background level (i.e. signal intensity is less than the signal threshold, namely no evidence of gene expression).

transcripts exhibit altered expression (Table 1). We used Probabilistic Neural Network (PNN) analyses to determine which transcript changes best discriminate control from SN50-treated explants. These analyses identified those transcripts with significant changes which are relatively more important in defining the SMG phenotype, regardless of the direction (up or down) of change.

Among the cell cycle transcripts with altered expression (Fig. 8A), PNN analysis shows that the *increased* expression of cyclin D2, p57, and Cdc25a, as well as *decreased* expression of PCNA, best discriminate control from SN50-treated explants. Cyclin D2, Cdc25a, and PCNA promote cell division; p57 inhibits cell division (Fig. 1). The significant decline in PCNA transcript (Table 1) is consistent with the highly significant ($p < 0.001$) decline in PCNA-defined cell proliferation (Fig. 4A).

Among apoptosis transcripts with altered expression (Fig. 8B), PNN analysis demonstrates that downregulated Caspase 1 transcript, almost alone, best discriminates control from SN50-treated explants. Caspase 1 activates Caspase 3 and appears to promote production of the cytokine IL-1β, which upregulates the transcription of both Caspases 1 and 3, additionally potentiating apoptosis [37,38]. Thus, *this* regulatory mechanism of caspase

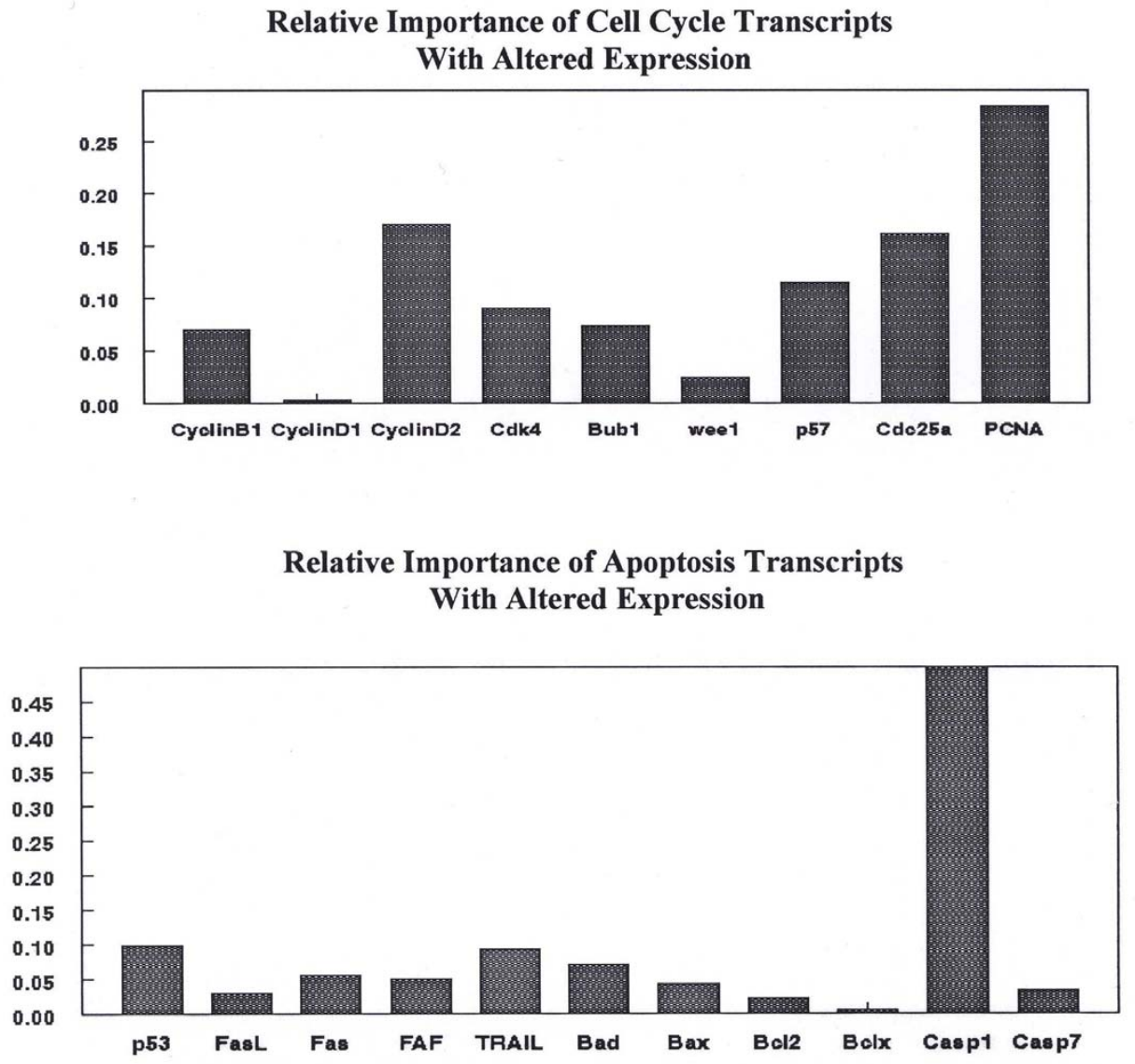

Figure 8
Relative importance of cell cycle and apoptosis transcripts with altered expression. The PNN analyses among cell cycle and apoptosis transcripts with altered expression identifies those transcripts which best discriminate control from SN50-treated E15 + 2 explants. Refer to Table 1 for the direction and magnitude of change for each transcript.

gene expression would likely be diminished in SN50-treated explants were they allowed to develop further in culture. Contemporaneous proteome analysis provides a very different profile (see Table 2 and text below).

Although many "Ras/Raf" growth factor pathway transcripts were upregulated (Table 1), as a group they were poor predictors of SMG phenotype (control v. SN50-treated). PNN analysis (Fig. 9A) shows that only IGF2, IGF2R, and IGFBP3 are best at discriminating control from SN50-treated explants.

TGF-β1 and TGF-β2 show a 2-fold increase (Table 1) which is not unexpected given that TGF-β and NF-κB are found to be inversely proportional to one another [39]. Nevertheless, among the TGF-β family transcripts and others related to their expression and signal transduction (Fig. 9B), BMP1, BMP3b, BMP8a, Smad7, and GR

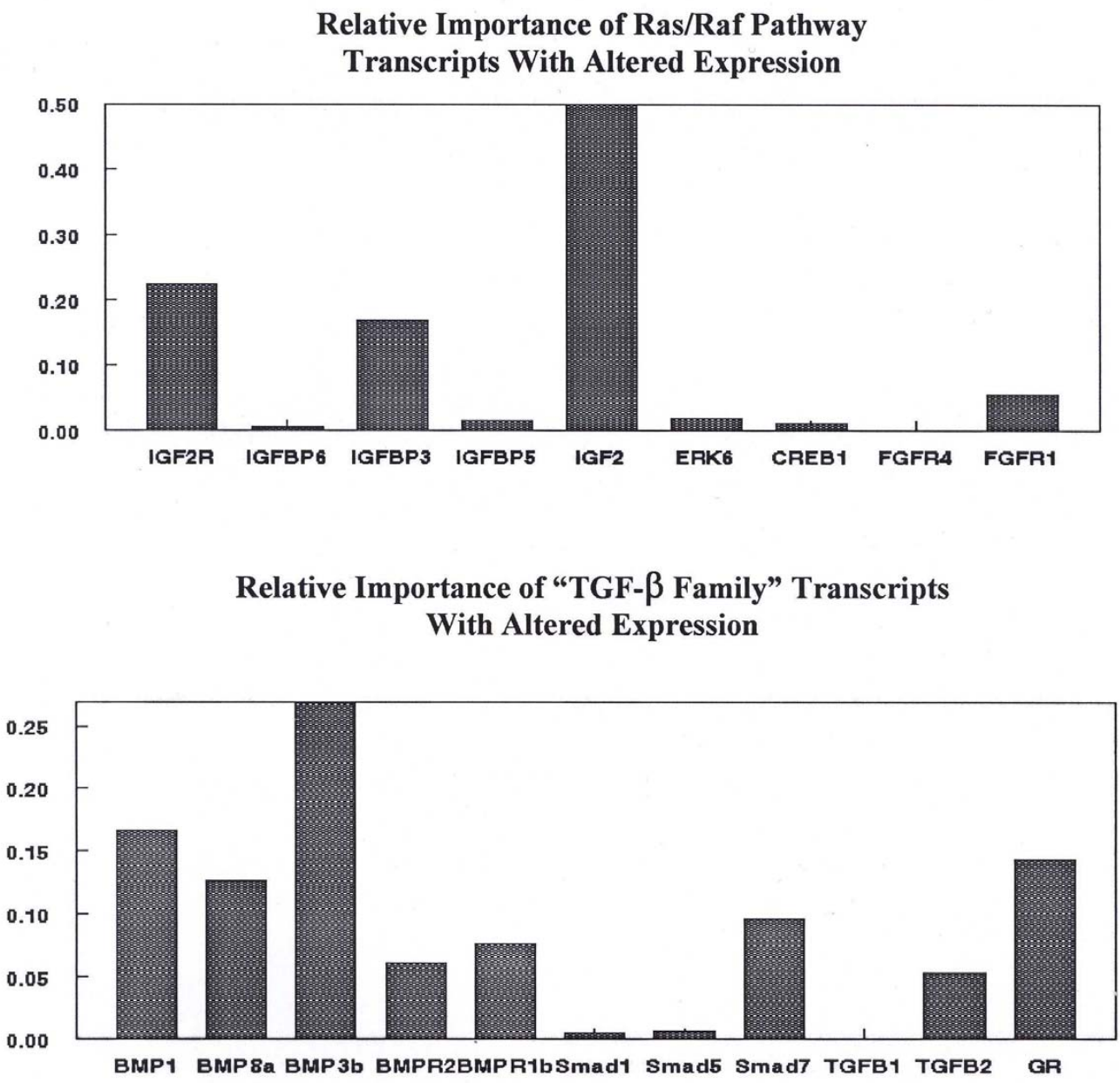

Figure 9
Relative importance of Ras/Raf family and "TGF-β-family" transcripts with altered expression. The PNN analyses among Ras/Raf family and "TGF-β-family" transcripts with altered expression identifies those transcripts which best discriminate control from SN50-treated E15 + 2 explants. Refer to Table 1 for the direction and magnitude of change for each transcript.

best discriminate control from SN50-treated explants. BMPs inhibit cell proliferation via downstream Smad1/5/8 proteins whereas Smad7 inhibits TGF-β and activin signaling (Fig. 1). This inhibition of TGF-β/activin signaling is modulated through NF-κB-dependent inhibition of Smad7 [40]. In addition, there is a negative feedback between NF-κB and Smad7; activated NF-κB inhibits Smad7 promotor activity [41] whereas Smad7 inhibits NF-κB activation and potentiates apoptosis [42]. Curiously, the *relative* importance of increased Smad7 expression is 20 times greater than that of Smad1/5 *vis.* defining the NF-κB-inhibited explants. It is likely that, in the absence of NF-κB's negative regulation, Smad7 signaling is upregulated, thereby sensitizing cells to apopto-

Table 1: Transcripts With Significant Changes In Expression After Inhibition Of NF-κB Nuclear Translocation*

Function (Fig. 1)	**Protein**	**Fold-Change**	**Function** (Fig. 1)	**Protein**	**Fold-Change**
Cell Cycle	PCNA	1.69↓	***Cell Cycle***	CyclinG1	1.99↑
	E2F3	1.86↑		CyclinG2	2.06↑
	CyclinA2	1.89↑		Cdk4	1.86↑
	CyclinB1	2.13↑		Cdc25a	2.00↑
	CyclinB2	1.91↑		Bub1	1.58↓
	CyclinD1	1.64↑		Bub1b	2.33↑
	CyclinD2	2.45↑		wee1	2.11↑
	CyclinE1	1.64↑		p57	2.05↑
Apoptosis	p53	1.54↑	***Apoptosis***	Bad	2.00↓
	Fas	1.79↑		Bax	1.82↑
	FasL	3.17↓		Bc12	1.58↑
	FAF	2.01↑		Bclx	1.58↑
	TRAIL	3.50↓		Caspase1	2.03↓
				Caspase7	1.90↓
Signal Transduction	IGF1	1.83↑	***Signal Transduction***	CREB1	1.91↑
	IGF2	2.33↑		c-jun	2.49↑
	IGF1R	1.53↑		c-myc	2.47↑
	IGF2R	1.69↑		TGF-β1	2.03↑
	IGFBP2	2.27↑		TGF-β2	2.06↑
	IGFBP3	2.41↑		BMP1	2.19↑
	IGFBP4	1.92↑		BMP3b	2.35↑
	IGFBP5	1.81↑		BMP8a	1.67↓
	IGFBP6	2.48↑		BMPR1b	1.92↓
	FGFR.1	2.93↑		BMPR2	1.87↑
	FGFR4	1.67↓		Smad1	1.90↑
	Ras	1.58↑		Smad5	1.50↑
	B-Raf	2.01↑		Smad7	1.97↑
	ERK6	2.02↑		GR	1.67↓

* This composite data represents the mean changes of 3 independent experiments.

sis. Finally, the nearly 2-fold decrease in glucocorticoid receptor (GR) is also of high relative importance in defining the SN50-treated phenotype (Table 1). Glucocorticoids (CORT) function through the GR to both activate specific gene expression as well as transrepress NF-κB [41]. Since GR confers this latter effect by associating through protein-protein interactions with NF-κB bound at κB response elements [43–47], it is important to also evaluate changes in GR protein levels (see below).

Further, we utilized PNN analysis to determine the iterated composite relative importance among *Connections Map* (Fig. 1) transcripts which have altered expression as a consequence of inhibition of NF-κB translocation into the nucleus (Fig. 10). That is, we then subjected those transcripts with altered expression in each group (cell cycle, apoptosis, Ras/Raf, TGF-β family) previously shown in Figures 7 and 8 to be relatively important in defining the SN50 SMG phenotype to further PNN analysis. This transciptomic analysis is a time-bound "snapshot" in which gene expression is indicative of possible future protein expression. It is instructive that, of the 53 *Connections Map* transcripts with altered expression (Table 1), 4 genes of diverse pathways but overlapping function best discriminate control from SN50-treated explants: PCNA, GR, BMP1, BMP3b. The declining PCNA and GR reflect the sharp decline in cell proliferation and branching; the increasing BMP1 and BMP3b similarly reflects inhibition of cell proliferation (Fig. 1).

Proteomic analysis

Our cDNA array analysis provides a *good first* approximation of *likely* protein differences. However, one cannot extrapolate from mRNA abundance to relevant protein levels [48]. A recent study by Aebersole and coworkers [48] analyzing yeast protein and mRNA abundance clearly showed that mRNA transcript levels are *poor* predictors of protein expression. They demonstrate

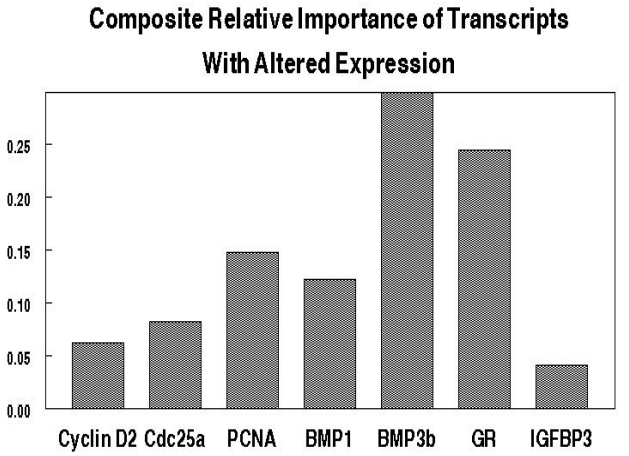

Figure 10
Iterated composite relative importance of all *Connections Map* transcripts with altered expression. Transcripts previously shown in Figures 8 and 9 to best discriminate control from SN50-treated explants were subjected to further PNN analysis to determine which transcripts are *most* discriminating in defining the SN50-treated E15 + 2 phenotype. Refer to Table 1 for the direction and magnitude of change for each transcript.

Table 2: Proteins With Significant Changes In Expression After Inhibition of NF-κB Nuclear Translocation*

Protein	**Fold-Change**	**Function** (Fig. 1)
PCNA	3.7↓	cell cycle
E2F1	4.1↑	cell cycle
Chk1	>5↑	cell cycle
Chk2	>5↑	cell cycle
FADD	>5↑	apoptosis
FAF	1.9↑	apoptosis
Caspase 6	>5↑	apoptosis
PARP	>5↑	apoptosis
Ras	1.9↑	signal transduction
c-Raf	>5↑	signal transduction
Mek2	>5↑	signal transduction
ERK1	1.6↓	signal transduction
ERK2	1.5↑	signal transduction
Rsk	2.4↑	signal transduction
JAK1	>5↑	signal transduction
STAT1	1.7↑	signal transduction
JNK1	>5↑	signal transduction
GR	1.8↓	signal transduction

* This composite data represents the mean changes of 2 independent samples.

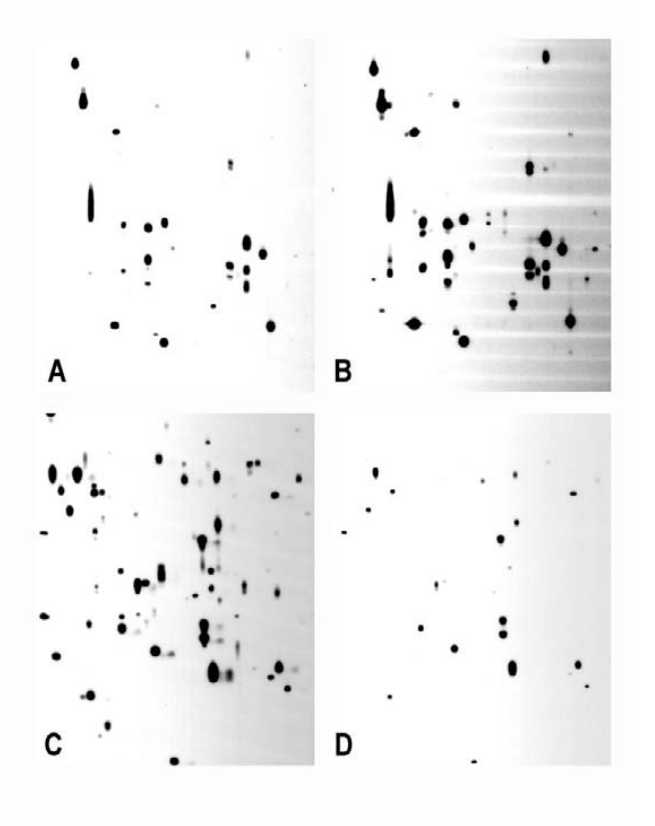

Figure 11
2-D Western blot multiprotein analyses of ~600 signal transduction and related proteins in E15+2 control and 100 μg/ml SN50-treated explants revealed significant changes in protein expression. Comparison of representative control (A, C) and SN50-treated (B, D) equivalent Western blots indicates marked qualitative and quantitative differences in the expression of specific signaling proteins with SN50 treatment compared to control.

that some genes with comparable mRNA levels exhibited a 20-fold difference in their protein expression while mRNA levels of comparable protein expression varied as much as 30-fold.

Thus, we next analyzed SN50-treated and control E15 + 2 SMG explants using 2-D Western Multiprotein Arrays to determine protein differences. This technique allows for the densitometric analysis of about 600 signal transduction and other proteins simultaneously in each independent sample (Fig. 11). As shown in Table 2, we find 18 proteins which have both a 1.5-fold or greater change with NF-κB inhibition *and* are specifically related to the *Connections Map* (Fig. 1). They include signal transduction, cell cycle, and apoptosis proteins that are either directly or indirectly downstream from activation of the TNF, IL-6, EGF, IGF, and FGF signaling pathways. The

significant decline in PCNA protein (Table 2) is consistent with the significant decline in PCNA transcript (Table 1) and PCNA-defined cell proliferation (Fig. 4A).

PNN analysis shows that among cell cycle proteins with altered expression (Fig. 12A), the increased expression of Chk1, Chk2, and E2F1 best discriminates control from SN50-treated explants. Of particular interest is E2F1. Among the five known mammalian E2Fs, the ability to induce apoptosis is unique to E2F1 [49]. Overexpression of E2F1 in several cell lines results in G_2 arrest, as well as apoptosis via p53-dependent and p53-independent pathways [50–52]. The presence of a dysplastic SMG phenotype in *E2f1*$^{-/-}$ mice indicates that E2F1 plays an important role during SMG development [53]. Moreover, E2F1 overexpression in human salivary gland (HSG) cells diverted these cells into an apoptotic pathway [54].

Among apoptosis proteins with altered expression (Fig. 12B), PNN analysis demonstrates that increased expression of FAF and Caspase 6 best discriminates control from SN50-treated explants. Caspase 6 is activated by active Caspase 3 and in turn cleaves lamin, resulting in nuclear membrane fragmentation [55]. FAF interacts with the cytoplasmic domain of the Fas receptor to potentiate Fas-mediated apoptosis [56,57]. Thus, the upregulated cell cycle inhibitors and apoptotic proteins clearly favor cell cycle arrest and death.

Among signal transduction proteins with altered expression (Fig. 12C), PNN analysis shows that members of all three growth factor pathways (Ras/Raf; JAK/STAT; JNK) have high relative importance in discriminating control from SN50-treated explants. Of particular note are c-Raf, ERK2, and JAK1. Raf plays a key role in the Ras signaling pathway (Fig. 1). That ERK2 is of very high relative importance is consistent with the observation that the MAPK/ERK overrides apoptotic signaling from Fas, TNF and TRAIL receptors [58]. It appears that effectors apart from the MAPK/ERK pathway may also mediate the anti-apoptotic function of c-Raf [55a]. Further, both the SHP-2/Ras and JAK/STAT3 pathways are activated by IL-6R/gp130 signaling (Fig. 1).

Moreover, it is especially noteworthy that the nearly 2-fold *decline* of glucocorticoid receptor (GR) (Table 2) is also of very high relative importance in defining SMGs deprived of NF-κB nuclear translocation. As noted above, CORT/GR binding both activates specific gene expression and transrepresses NF-κB [47]. To repress NF-κB, the GR associates through protein-protein interactions with NF-κB bound at κB response elements [44–47]. The precise relationship between decreased NF-κB-mediated transcription and a decreased GR protein expression is unclear.

Nevertheless, CORT/GR function is important to embryonic SMG morphogenesis [60]. Radioimmunoassays first detect SMG CORT in amounts >2 pg/gland on E15; Western analysis first detects SMG GR on E14 (0.14 fmol/gland). By E18, SMG CORT has increased more than 50-fold, and SMG GR has increased nearly 11-fold. The SMG GR is functional, as defined by its ability to bind a DNA response element (GRE). Increasing CORT/GR function *in vivo* is associated with a significant decline in TGF-β expression and a significant increase in cell division. SMG primordia cultured under serumless, chemically defined conditions, and deprived of CORT, exhibit a dramatic decline of SMG branching morphogenesis. It is reasonable, then, to assume that the high relative importance of diminished GR protein expression to the phenotype of SN50-treated SMGs is directly related to the significant ($p < 0.001$) decline in cell proliferation and branching (Fig. 3A, B; Fig. 4A).

The iterated composite relative importance of all *Connections Map* proteins with altered expression as a consequence of NF-κB inhibition was then determined (Fig. 13). This proteomic analysis is a time-based "snapshot" of proteins assumed to be associated with physiologic function at the moment of SMG harvesting. Viewing the most defining proteins with altered expression, it is clearly reflective of increased apoptosis (increased Chk1, Caspase 6, E2F1), decreased cell proliferation and branching (decreased GR), and, interestingly, increased expression of diverse signal transduction pathways (Ras/Raf/ERK, JNK) to compensate for the proapoptotic signal.

Analysis of activated pathway components

We then focused our attention on two particularly important pathways relative to cell proliferation and apoptosis, ERK 1/2 and Caspase 3. Downstream of activated ERK 1/2 is an upregulation of cell proliferation proteins and potentially enhanced cell division, as well as a protective effect over apoptotic signaling via suppressed activation of caspase effectors. Downstream of activated Caspase 3 are the sequellae of apoptosis, including PARP cleavage and inhibition of DNA repair, DNA fragmentation, and nuclear membrane fragmentation. The increase or decrease in expression of the components of any signaling pathway is not necessarily probative of pathway activity. Rather, it is the change in the level of activated protein that is physiologically important. Thus, we determined if SN50 treatment was associated with activation of the ERK1/2 and Caspase 3 pathways, using E15 + 2 control and SN50-treated explants, 1-D Western blot analysis, and antibodies specific to activated (phosphorylated/cleaved) proteins. Specifically, we evaluated the levels of activated c-Raf, ERK1/2, Caspase 3, and PARP using antibodies which identify only the phospho-

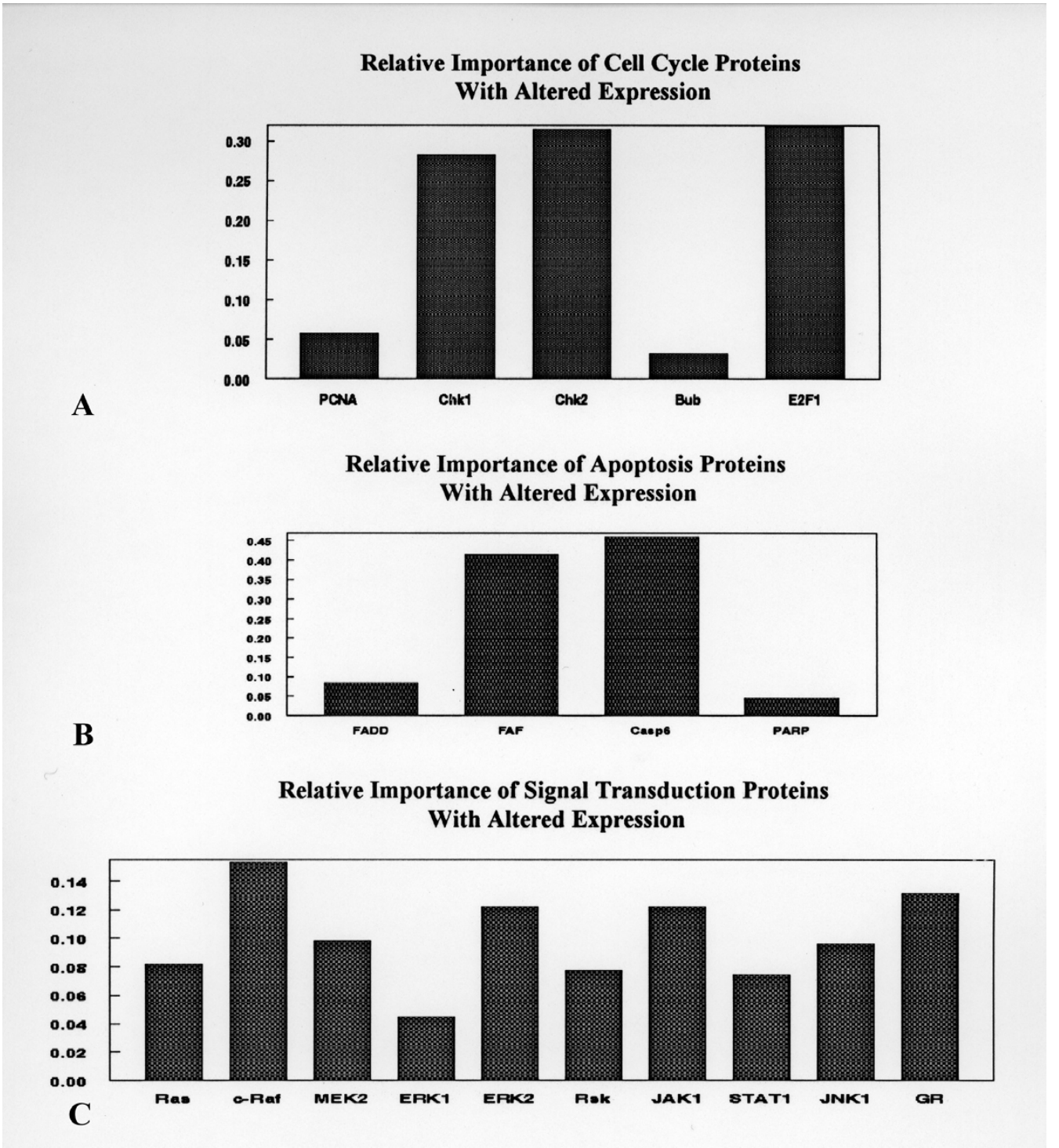

Figure 12
Relative importance of cell cycle, apoptosis, and signal transduction proteins with altered expression in defining control and SN50-treated phenotypes. These PNN analyses among cell cycle, apoptosis, or signal transduction proteins with altered expression identified which proteins best discriminate control from SN50-treated E15 + 2 explants. Refer to Table 2 for the direction and magnitude of change for each protein.

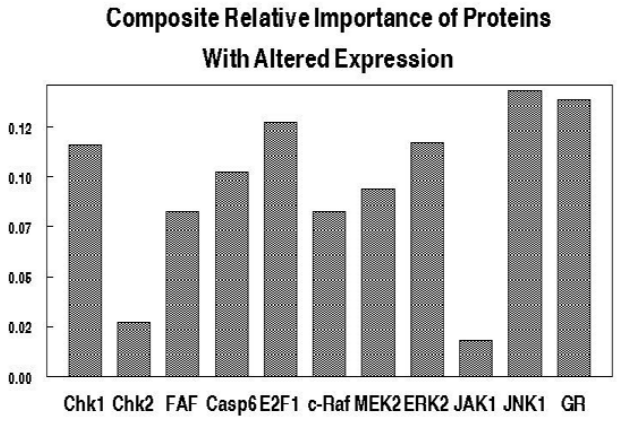

Figure 13
Iterated composite relative importance of all *Connections Map* proteins with altered expression. Proteins previously shown in Figures 11 and 12 to best discriminate control from SN50-treated explants were subjected to further PNN analysis to determine which proteins are *most* discriminating in defining the SN50-treated E15 + 2 phenotype. Refer to Table 2 for the direction and magnitude of change for each protein.

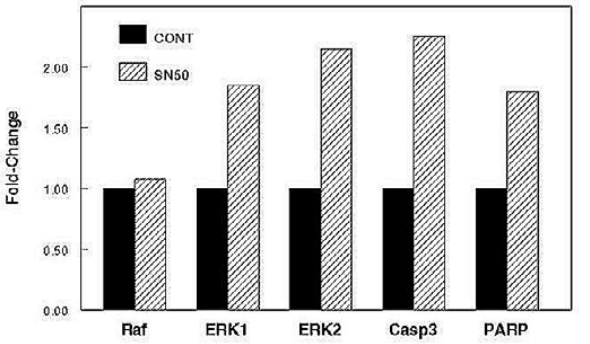

Figure 14
SN50-treatment induces the ERK1/2 and Caspase 3 pathways. Quantitation of *phospho*-ERK1/2, *phospho*-cRaf, *cleaved* Caspase 3, and *cleaved* PARP protein expression in control (CONT) and 100 μg/ml SN50-treated E15 + 2 explants. Two independent experiments were conducted and the results are presented as a mean fold change relative to control protein. SN50 treatment induced a significant increase in *activated* ERK 1/2, Caspase 3, and PARP levels compared to control; no change was seen in *activated* c-Raf level.

rylated or cleaved proteins and do not cross react with the inactive protein. We found a significant increase ($p < 0.05$) in activated ERK1/2, Caspase 3, and PARP in SN50-treated explants (Fig. 14); no change was seen in activated c-Raf levels between control and SN50-treated explants. The greater than 2-fold increase in Caspase 3 activation is associated with a 1.8-fold increase in PARP cleavage (Fig. 14) and a 10-fold increase in apoptosis (Fig. 4B). Since Caspase 3 is nodal to E2F1 (via p53), FAF (via Fas/Caspase 8), and Caspase 6 [33,36,37,39], our observation of increased activated Caspase 3 is consistent with the increased levels of E2F1, FAF, and Caspase 6 proteins (Table 2). Regarding the ERK1/2 pathway, we found a greater than 2-fold increase of activated ERK2 in SN50-treated glands (Fig. 13) associated with a 1.5-fold increase in total ERK2 protein (Table 2). This increased activity of proapoptotic (caspase3/PARP) and compensatory antiapoptotic (ERK1/2) pathways is consistent with the dramatic cell death seen in SN50-treated SMGs. Paradoxically, increased ERK1 activation is seen despite a 1.6-fold decrease in total ERK1 protein (Table 2) and increased ERK 1/2 activation is associated with virtually no change in the antecedent activation of c-Raf. The latter is consistent with the demonstration that c-Raf function is not mediated by the MAPK/ERK cascade [59]. Moreover, although we find an increase in total Raf protein (Table 2), no increase in activated c-Raf is found; we also see a 2-fold increase in activated Caspase 3 but no change in total Caspase 3 protein. These results clearly illustrate that changes in total protein level are not always indicative of altered protein activity.

Finally, it should be noted that a recent study using cell lines raised the possibility that SN50's action is not specific to NF-κB [61,62]. SN50 is composed of the NLS for NF-κB p50 and was believed to specifically block NF-κB p50/p65 nuclear translocation by binding the NLS receptor complex and preventing transport through the nuclear pore [33–35]. However, Torgerson and coworkers [61] have shown that SN50 treatment inhibited nuclear transport of transcription factors NFAT, AP-1, STAT1, and NF-κB at a high dose of 210 μg/ml in Junkrat cells. However, others have shown that lower doses ≤ 100 μg/ml of SN50 specifically inhibited NF-κB nuclear translocation in human peripheral blood lymphocytes and murine T cells [33,63]. These reported differences are likely due to dose-dependent or cell-specific differences in the effect of SN50 [64]. Given that: (1) embryonic SMGs were cultured in the presence of 100 μg/ml SN50, (2) immunodetectable NF-κB was absent from SMG epithelia nuclei in TNF + SN50-treated explants, and (3) one cannot extrapolate observations in Jurkat cells to those in primary cells [64] or organ cultures, it is most probable that our observed interruption of SMG development is proximately due exclusively to the inhibi-

tion of NF-κB nuclear translocation. Indeed, for low doses of SN50, there is no evidence in the literature to the contrary. Nonetheless, we do recognize that absence of evidence is not necessarily evidence of absence.

Conclusions

Our results indicate that NF-κB-mediated transcription is directly or indirectly critical to embryonic SMG developmental homeostasis. We demonstrate the interplay between gene expression, protein expression, protein activity, and morphology in response to NF-κB inhibition. Gene/protein differences between control and NF-κB-inhibited phenotypes are not linearly causal of SMG dysplasia. In fact, these differences are discovered correlations between network components and an emerging SMG phenotype, a glimpse of nonlinear organogenesis [65].

Considering the outcome of this study relative to the *Connections Map* (Fig. 1), it is apparent that NF-κB nuclear translocation is functionally integral to a genetic network with broadly related, rather than independent, components. It may be said to represent the collective dynamics of a "small-world" network such that the average number of factors in the shortest chain connecting any two factors is small [66]. Such dynamical systems with small-world coupling display enhanced signal-propagation speed and synchronizability. Thus, if one focuses on the superimposition of the various layers of information, namely morphology, gene expression, protein expression, and protein activity (Figs. 3,4,5,6,7,8,9,10,11,12,13,14), one can visualize a coordinated, multidimensional response to inhibited NF-κB nuclear translocation. This visualization, however, is necessarily impressionistic even though our assays have some precision. This is so because we cannot extrapolate from transcriptome to proteome to activated proteins with any accuracy (in the absence of actual steady-state measures), *and* because in these experiments time is necessarily cross-sectional, not longitudinal. Nevertheless, relative to understanding a complex genetic network and organogenesis, our results demonstrate the importance of contemporaneously evaluating the gene, protein, *and* activated protein expression of multiple components from multiple pathways within broad functional categories. Understanding the signal dynamics of these pathways will require expanded models that encompass more aspects of regulation [e.g. [67]]. Still, we will always be limited by the fact that phenotypes are complex, emergent phenomena [16].

Materials and Methods

Tissue collection

Female B10A/SnSg mice, obtained from Jackson Laboratories (Bar Harbor, ME), were maintained and mated as previously described [60]; plug day = day 0 of gestation. Pregnant females were anesthetized on days 15–19 of gestation (E15–18) with methoxyflurane (metafane) and euthanized by cervical dislocation. Embryos were dissected in cold phosphate buffered saline (PBS) and staged according to Theiler [68]. SMGs were dissected and cultured, processed for histology, or stored at -70°C. For cDNA expression and proteomic studies, E15 + 2 explants were collected, pooled, and stored at -70°C.

Culture system

E15 SMG (mostly *Canalicular* Stage) primordia were cultured using a modified Trowell method as previously described [13]. The medium consisted of BGJb (Life Technologies, Rockville, MD) supplemented with 0.5 mg ascorbic acid/ml and 50 units penicillin/streptomycin (Life Technologies), pH 7.2, and replicate cultures were changed every other day. Cultures were supplemented on day 0 and maintained for the duration of the experiments. In each of the enumerated studies, a minimum of 12 explants were cultured for 2 or 4 days in the cell permeable peptide SN50 (Biomol Research, Plymouth Meeting, PA) which inhibits NF-κB translocation into the nucleus [24,33–35]. The concentration used (100 μg/ml) was double that shown to inhibit NF-κB translocation in mouse endothelial LE-II cells; 100 μg/ml mutant SN50 (mSN50) peptide was used as a *positive* control and control BGJb medium as a *negative* control. We evaluated their microanatomy by routine hematoxylin and eosin histology. We report a marked difference between SN50-treated and control explants or SN50- and mSN50 peptide-treated explants. No differences were observed between control and mSN50-treated explants. Since these initial studies demonstrated no difference between explants cultured in control media alone and in mutant peptide, control media was used as the control in all subsequent experiments. Ten independent experiments of E15 primordia were cultured for 2 days (E15 + 2) in CONT (control) or SN50-supplemented media, each group consisting of a minimum of 8 explants per group. E15+2 explants were collected and processed as described below.

To further demonstrate that SN50 treatment inhibited NB-κB activation, we evaluated if TNF supplementation would induce NF-κB translocation and SMG morphogenesis. E15 SMGs were cultured for 4 days or longer in 10 U/ml recombinant mouse TNF (rTNF, R & D, Minneapolis, MN), 100 μg/ml SN50 + 10 U/ml rTNF, or 100 μg/ml mSN50 + 10 U/ml rTNF, 6–10 explants per treatment group. This rTNF concentration was previously shown in our laboratory to induce embryonic SMG morphogenesis and cell proliferation [13]. Explants were collected and evaluated by histological and immunochemical analyses as described below.

Histology and immunolocalization

SMGs were fixed in Carnoy's fixative, processed, embedded in low-melting point paraplast, and stored for brief periods at 4°C as previously described [13]. Cultured explant morphogenesis was analyzed by dissecting microscopy and by light microscopy of serial sections stained with hematoxylin and eosin. A minimum of 5 explants per group was evaluated for all experimental groups. For immunochemistry, the tissues were sectioned at 7 μm, placed on cleaned, gelatin-coated slides at 37°C for 3 hr, and immediately immunostained as previously described [9,13]. The sections were incubated in polyclonal goat anti-NF-κB p65/RelA antibody (C-20)(Santa Cruz Biotechnology, Santa Cruz, CA); this antibody has been shown to cross-react with mouse p65; it is not cross-reactive with RelB p68 or c-Rel p75. We confirmed the spatial distribution of NF-κB using a polyclonal goat anti-NF-κB p50 antibody (C-19) (Santa Cruz Biotechnology); this antibody has been shown to react with mouse p50 or p105; it is not cross-reactive with NF-κB p52, p65/RelA or p100. Controls consisted of sections incubated with preimmune serum or in the absence of primary antibody; controls were routinely negative. The spatial distribution of NF-κB p65 was identical to that of NF-κB p50. Therefore, we only show the results of the anti-NF-κB p65 antibody experiments.

Quantitation of activated p53

To quantitate differences in *activated* (phosphorylated) p53 protein, 3 SN50 and control E15 + 2 explants were sectioned, preincubated with unlabeled goat-anti mouse IgG as previously described [9] and sequentially incubated with a monoclonal anti-phosphorylated p53 (Ser15) antibody (Cell Signaling Technology, Beverly, MA), biotin-labeled goat anti-mouse IgG, and HRP-labeled SA (Zymed Laboratories, South San Francisco, CA), and counterstained with hematoxylin. Controls consisted of preimmune serum or PBS alone. In this set of experiments, the cytoplasm appears blue and *activated* p53-positive cells appear dark brown. Three sections per group were selected and 3 areas per section was photographed at 200×. p53-positive epithelial cells/total epithelial cells were determined per area and the mean ratios per section and per group were determined. Statistical comparisons were made between CONT and SN50-treated E15 + 2 explants as described below.

Cell proliferation assay

E15 + 2 CONT or SN50-treated explants were sectioned, incubated with anti-PCNA using the Zymed mouse PCNA kit (South San Francisco, CA), and counterstained with hematoxylin as previously described [13]. In this set of experiments, the cytoplasm appears blue and PCNA-positive cells appear dark brown. Quantitation of cell proliferation was conducted as described above for p53. Cell proliferation is presented as the ratio of PCNA-positive epithelial cells/total epithelial cells. Mean ratios per section and mean ratios per group were determined. Statistical comparisons were made between CONT and SN50-treated E15 + 2 explants as described below.

Apoptosis assay

Apoptotic cells were detected using a monoclonal antibody to single-stranded DNA (ssDNA) (Mab F7–26) according to the method of Apostain, Inc. (Miami, FL) [13]. Selective binding of anti-ssDNA monoclonal antibody F7–26 to *apoptotic nuclei* reflects decreased stability of DNA to thermal denaturation. Four positive and negative controls were conducted. *Negative controls:* (1) Tissue sections were heated and treated with S1 nuclease (Sigma); S1 nuclease eliminates staining of apoptotic cells, thus demonstrating that Mab F7–26 binds specifically to ssDNA. (2) Sections were pretreated in PBS containing lysine-rich histone (Sigma) prior to heating and immunostaining; reconstitution with histone restores DNA stability in apoptotic nuclei, thus preventing DNA denaturation and eliminating Mab staining of apoptotic cells. *Positive controls:* (1) Sections were heated in water and treated with Mab; bright staining of all non-apoptotic nuclei with low apoptotic indexes demonstrates that the procedure is adequate to detect ssDNA. (2) Sections were pretreated with proteinase K before heating; intensive staining of non-apoptotic nuclei demonstrates that the procedure detects decreased DNA stability induced by the digestion of nuclear proteins. Mab F7–26 was purchased from Apostain, Inc.

Apoptotic nuclei appear as dark brown. Since the sections were not counterstained with hematoxylin in this set of experiments, epithelial cell cytoplasm appears as light brown. Only apoptotic (variously intense dark brown) nuclei were counted in control and SN50-treated sections. Apoptosis was evaluated in a minimum of 4 explants per experimental group. Quantitation of apoptotic nuclei was conducted as described above for p53. Apoptosis is presented as the ratio of apoptotic-positive epithelial cell nuclei/total epithelial cell nuclei. Mean ratios per section and mean ratios per group were determined. Statistical comparisons were made between CONT and SN50-treated E15 + 2 explants as described below.

cDNA expression arrays

For cDNA Expression Array analysis, E15 SMG primordia were cultured in the presence or absence of SN50 peptide for 2 days (E15 + 2), collected in cold PBS containing 0.02% DEPC, snap frozen, and stored at -70°C. Clontech (Clontech Laboratories, Inc., Palo Alto, CA) Mouse 1.2 cDNA Expression Arrays were used to analyze each sample. These arrays include 1176 mouse cDNAs, 9 housekeeping control cDNAs, and negative controls im-

mobilized on a nylon membrane [www.clontech.com] . Briefly, total RNA was isolated and cDNA probes were synthesized using the Atlas Pure Total RNA Labeling System and ^{32}P. The labeled cDNA probes were hybridized to the Atlas Array using ExpressHyb Solution. Hybridization signals were revealed by phosphorimaging and quantitated using the Clontech Atlas Image 1.01 software package, which allows for unbiased normalization of transcript abundance to overall signal. We generated pseudocolored images indicating up and down gene regulation. The probe set intensity (average difference) is proportional to the abundance of the specific mRNA it represents and was calculated by comparing hybridization signal of the control oligonucleotide to that of the treated. Total signal intensity of different probes was scaled to the same value before comparison. Fold changes were calculated by AtlasImage 1.0 software by pairwise comparisons of corresponding probe pairs from experimental and control. Three independent experiments were conducted per experimental group and the composite array determined. Relevant genes with altered expression were then assigned to functional groups. Specifically, we assigned those genes related to the *Connections Map* (Fig. 1) that have a 1.5 or greater fold-change to functional groups (*i.e.,* cell cycle, apoptosis, signal transduction, etc.) which have biological significance.

2-D western array screening

The expression of signaling proteins was analyzed by Powerblot Western Array Screening (BD Transduction Laboratories, Lexington, KY). This 2-D Western Blot Array methodology simultaneously examines relative changes in protein expression in ~600 proteins in a given sample. Using highly specific monoclonal antibodies in antibody combinations carefully formulated by BD Transduction Laboratories, this multiprotein assay detects proteins to the nanogram levels and can distinguish closely related members of many important signaling families. E15+2 CONT and SN50-treated explants were collected and processed according to the protocol of BD Transduction Laboratories. Each sample (CONT and SN50-treated) was analyzed on 4 separate 2-D gels which were then transferred onto 4 blots. Each blot was then incubated with a different mixture of ~150 monoclonal antibodies and proteins were detected by chemiluminescence; ~600 (150 antibodies × 4 blots) proteins were evaluated in a given sample. For this set of experiments, two independent samples were analyzed The relative level of proteins were determined by phosphor imaging and normalized to overall signal. We then assigned those *Connections Map* proteins with a 1.5 or greater fold-change to functional groups as described above.

1-D western blot analysis

To determine which key pathways were activated, Western blot analyses of phosphorylated or cleaved proteins in E15+2 CONT and SN50-treated explants were conducted as previously described [5]. For this set of experiments, we first determined the specificity for each of the following antibodies purchased from Cell Signaling Technology (Beverly, MA) using E15 and E17 SMG homogenates: anti-phosphorylated Erk1/2 [phospho-p44/42 MAP kinase (Thr202/Tyr204)] antibody, anti-phosphorylated c-Raf(Ser259) antibody, anti-cleaved Caspase 3 (D 175) antibody, and anti-cleaved PARP (D214) antibody. Each antibody had previously been shown to be specific for the activated (phosphorylated/cleaved) protein and not to cross react with inactive protein. Once optimal experimental conditions were established for each antibody, we then incubated blots of E15 and E17 SMGs in a mixture of these 4 antibodies and determined that we could identify all proteins in a single sample by M_r. This methodology using a mixture of antibodies has been successfully used by Cell Signaling Technology and BD Signal Transduction for 2-D and 1-D Western blot analyses. Controls consisted of blots incubated in preimmune rabbit serum or in the absence of primary antibodies; controls were routinely negative. In each sample, each *activated* protein was identified by M_r and the relative level of *activated* proteins in CONT and SN50-treated explants was determined by densitometry. The SN50 results are presented as fold change relative to CONT protein. Two independent samples per group was analyzed. Statistical comparisons were made between CONT and SN50-treated E15 + 2 explants as described below.

Probabilistic neural network analysis

We used PNN analyses to determine which *Connection Map* (Fig. 1) transcripts or proteins with altered expression best discriminate CONT from SN50-treated explants with 100% sensitivity and specificity [69]. PNN analyses identify the relative importance (0–1, with 0 being of no relative importance and 1 being relatively most important) of gene and protein expression changes in defining the SN50 phenotype. It is the change in expression, not the direction of change, that is important in defining the phenotype. The algorithm we used (Ward Systems Group, Frederick, MD) is based upon the work of Specht and colleagues [69–72]. Utilizing proprietary software designed by Ward Systems Group (Frederick, MD), we made comparisons among *Connections Map* transcripts or proteins with altered expression in a given group.

Statistical analysis

Means differences were analyzed by t-test in the usual manner [73]. To meet the assumptions of this analysis, namely normality and homoscedasticity (homogeneity

of variances), counts, ratios, and percentages were log or arcsin transformed [74]. This allows for parametric statistical testing.

Acknowledgments

Supported by NIH grant DE 11942

References

1. Ball WD: **Development of the rat salivary glands. III. Mesenchymal specificity in the morphogenesis of the embryonic submaxillary and sublingual glands of the rat.** *J Exp Zool* 1974, **188**:277-288
2. Cutler LS, Gremski W: **Epithelial-mesenchymal interactions in the development of salivary glands.** *Crit Rev Oral Biol Med* 1991, **2**:1-12
3. Denny PC, Ball WD, Redman RS: **Salivary glands: a paradigm for diversity of gland development.** *Crit Rev Oral Biol Med* 1997, **8**:51-75
4. Gresik EW, Kashimata M, Kadoya Y, Yamashina S: **The EGF system in fetal development.** *Eur J Morphol* 1998, **36 (Suppl)**:92-97
5. Jaskoll T, Chen H, Denny P, Denny P, Melnick M: **Mouse submandibular gland mucin: embryo-specific mRNA and protein species.** *Mech Dev* 1998, **74**:179-183
6. Kashimata M, Sayeed S, Ka A, Onetti-Muda A, Sakagami H, Faraggiana T, Gresik E: **The ERK-1/2 signaling pathway is involved in the stimulation of branching morphogenesis of fetal mouse submandibular glands by EGF.** *Dev Biol* 2000, **220**:183-196
7. Redman RS: **Development of the salivary glands.** *In The Salivary System. Edited by Sreebny LM. Boca Raton: CRC Press* 19871-20
8. Wessells N: *Tissue interactions and development. Menlo Park: Benjamin Cummins,* 1977
9. Jaskoll T, Melnick M: **Submandibular gland morphogenesis: stage-specific expression of TGF-alpha, EGF, IGF, TGF-beta, TNF and IL-6 signal transduction in normal mice and the phenotypic effects of TGF-beta2, TGF-beta3, and EGF-R null mutations.** *Anat Rec* 1999, **256**:252-268
10. Jaskoll T, Zhou Y-M, Chai Y, Makarenkova HP, Collinson JM, West JD, Lee J, Melnick M: **Embryonic submandibular gland morphogenesis: stage-specific protein localization of FGFs, BMPs, Pax6 and Pax9 in normal mice and abnormal SMG phenotypes in FgfR2-IIIc+/Δ, BMP7-/- and Pax6-/- mice.** *Cells Tiss Org* 2002, **270**:83-98
11. Kashimata M, Gresik E: **Epidermal growth factor system is a physiological regulator of development of the mouse fetal submandibular gland and regulates expression of the α6-integrin subunit.** *Dev Dyn* 1997, **208**:149-161
12. Melnick M, Jaskoll T: **Mouse submandibular gland morphogenesis: a paradigm for embryonic signal processing.** *Crit Rev Oral Biol* 2000, **11**:199-215
13. Melnick M, Chen H, Zhou Y-M, Jaskoll T: **Embryonic mouse submandibular salivary gland morphogenesis and the TNF/TNF-R1 signal transduction pathway.** *Anat Rec* 2001, **262**:318-320
14. Melnick M, Chen H, Zhou Y, Jaskoll T: **Interleukin-6 signaling and embryonic mouse submandibular salivary gland morphogenesis.** *Cells Tiss Org* 2001, **168**:233-245
15. Bhalla U, Iyengar R: **Emergent properties of networks of biological signaling pathways.** *Science* 1999, **283**:381-386
16. Kauffman SA: *The origins of order. New York: Oxford University Press,* 1993
17. Kauffman SA: *At Home in the Universe. The Search for Laws of Self-Organization and Complexity. New York: Oxford University Press,* 1995
18. Jordan JD, Landau EM, Iyengar R: **Signaling networks: the origins of cellular multitasking.** *Cell* 2000, **103**:193-200
19. Gilbert SF, Sarkar S: **Embracing complexity: organicism for the 21st century.** *Dev Dyn* 2000, **219**:1-9
20. Palsson B: **The challenges of in silico biology.** *Nature Biotech* 2000, **18**:1147-1150
21. Smith RD: **Probing proteomes-seeing the whole picture?** *Nature Biotech* 2000, **18**:1041-1042
22. Streelman JT, Kocher TD: **From phenotype to genotype.** *Evol Dev* 2000, **2**:166-173
23. Ghosh S: **Regulation of inducible gene expression by the transcription factor NF-kappaB.** *Immunol Res* 1999, **19**:183-189
24. Maggirwar SB, Sarmiere PD, Dewhurst S, Freeman RS: **Nerve growth factor-dependent activation of NFκB contributes to survival of sympathetic neurons.** *J Neurosci* 1998, **18**:10356-10365
25. Qin ZH, Chen RW, Wang Y, Nakai M, Chuang DM, Chase TN: **Nuclear factor κB nuclear translocation upregulates c-Myc and p53 expression during NADA receptor-mediated apoptosis in rat seriatim.** *J Neurosci* 1999, **19**:4023-4033
26. Nishikimi A, Mukai J, Yamada M: **Nuclear translocation of nuclear factor kappa B in early 1-cell mouse embryos.** *Biol Reprod* 1999, **60**:1536-1541
27. Schmidt-Ullrich R, Memet S, Lilienbaum A, Feuillard J, Raphael M, Israel A: **NFκB activity in transgenic mice: developmental regulation and tissue specificity.** *Development* 1996, **122**:2117-2128
28. Pahl HL: **Activators and target genes of Rel/NFκB transcription factors.** *Oncogene* 1999, **18**:6853-6866
29. Perkins ND: **Achieving transcriptional specificity with NFκB.** *Int J Biochem Cell Biol* 1997, **29**:1433-1448
30. Wang CY, Mayo MW, Korneluk RG, Goeddel DV, Baldwin AS: **NFκB antiapoptosis: induction of TRAF1 and TRAF2 and c-IAP1 and c-IAP2 to suppress Caspase-8 activation.** *Science* 1998, **281**:1680-1683
31. Webster GA, Perkins ND: **Transcriptional crosstalk between NFκB and p53.** *Mol Cell Biol* 1999, **19**:3485-3495
32. Pise-Masison CA, Mahieux R, Jiang H, Ashcroft M, Radonivich M, Duvall J, Guillerm C, Brady JN: **Inactivation of p53 by Human T-cell lymphotropic virus Type 1 Tax requires activation of the NF-κB pathway and is dependent on p53 phosphorylation.** *Mol Cell Biol* 2000, **20**:3377-3386
33. Kolenko V, Bloom T, Rayman P, Bukowski R, Hsi E, Finke J: **Inhibition of NFκB activity in human T lymphocytes induces caspase-dependent apoptosis without detectable activation of Caspase-1 and -3.** *J Immunol* 1999, **163**:590-598
34. Lin YZ, SY Yao, Veach RA, Torgerson TR, Hawiger J: **Inhibition of nuclear translocation of transcription factor NF-κB by a synthetic peptide containing a cell-membrane permeable motif and nuclear localization sequence.** *J Biol Chem* 1995, **270**:14255-14258
35. Liu RY, Fan C, Olashaw NE, Wang X, Zuckerman KS: **Tumor necrosis factor-alpha-induced proliferation of human Mo7e leukemic cells occurs via activation of nuclear factor κB transcription factor.** *J Biol Chem* 1998, **274**:13877-13885
36. Ashkenazi A, Dixit V: **Death receptors: signaling and modulation.** *Science* 1998, **281**:1305-1308
37. Li M, Ona VO, Guegan C, Chen M, Jackson-Lewis V, Andrews LJ, Olszewski AJ, Stieg PE, Lee JP, Przedborski S, Friedlander RM: **Functional role of caspase-1 and caspase-3 in an ALS transgenic mouse model.** *Science* 2000, **288**:335-339
38. Monell C: *Caspase cascade in apoptosis. Biocarta* 2001 [www.biocarta.coni/pathfiles/caspasePathway.asp.]
39. Kaltschmidt B, Kaltschmidt C: **DNA array analysis of the developing cerebellum: transforming growth factor-β2 inhibits constitutively activated NFκB in granule neurons.** *Mech Dev* 2001, **101**:11-19
40. Bitzer M, von Gersdorff G, Liang D, Dominguez-Rosales A, Beg AA, Rojkind M, Bottinger EP: **A mechanism of suppression of TGF-beta/SMAD signaling by NF-kappa B/RelA** *Genes Develop* 2000, **14**:187-197
41. Nagarajan RP, Chen F, Li W, Vig E, Harrington MA, Nakshatri H, Chen Y: **Repression of transforming-growth-factor-β-mediated transcription by nuclear factor κB.** *Biochem J* 2000, **348**:591-596
42. Lallemand F, Mazars A, Prunier C, Bertrand F, Kornprost M, Gallea S, Roman-Roman S, Cherqui G, Atfi A: **Smad7 inhibits the survival nuclear factor κB and potentiates apoptosis in epithelial cells.** *Oncogene* 2001, **20**:879-884
43. Tao Y, Williams-Skipp C, Scheinman RI: **Mapping of glucocorticoid receptor DNA binding domain surfaces contributing to transrepression of NF-κB and induction of apoptosis.** *J Biol Chem* 2001, **276**:2329-2332
44. Doucas V, Shi Y, Miyamoto S, West A, Verma I, Evans RM: **Cytoplasmic catalytic subunit of protein kinase A mediates cross-repression by NF-κB and the glucocorticoid receptor.** *Proc Natl Acad Sci (USA)* 2000, **97**:11893-11898
45. McKay LI, Cidlowski JA: **CBP (CREB Binding Protein) integrates NF-κB (Nuclear Factor-κB) and glucocorticoid recep-**

tor physical interactions and antagonism. *Mol End* 2000, **14**:1222-1234
46. Nissen RM, Yamamoto KR: **The glucocorticoid receptor inhibits NFκB by interfering with serine-2 phosphorylation of the RNA polymerase II carboxy-terminal domain.** *Genes Dev* 2000, **14**:2314-2329
47. Wissink S, van Hairdo EC, vanned der Burg B, van der SAA PT: **A dual mechanism mediates repression of NF-kappa B activity by glucocorticoids.** *Mol Endocr* 1998, **12**:355-363
48. Gygi SP, Rochan Y, Franza BR, Aebersold R: **Correlation between protein and mRNA abundance in yeast.** *Mol Cell Biol* 1999, **19**:1720-1730
49. DeGregori J, Leone G, Miron A, Jakoi L, Nevins JR: **Distinct roles of E2F proteins in cell growth control including a unique role for the E2F1 protein as a signal as apoptosis.** *Proc Natl Acad Sci USA* 1997, **94**:7245-7250
50. Marzio G, Wagener C, Gutierrez MI, Cartwright P, Helin K, Giacca M: **E2F family members are differentially regulated by reversible acetylation.** *J Biol Chem* 2000, **275**:10887-92
51. Irwin M, Marin MC, Phillips AC, *et al*: **Role for the p53 homologue p73 in E2F1-induced apoptosis.** *Nature* 2000, **407**:645-648
52. Yang HL, Dong YB, Elliott MJ, Liu TJ, McMasters KM: **Caspase activation and changes in Bc1-2 family member protein expression associated with E2F1-mediated apoptosis in human esophageal cancer cells.** *Clin Can Res* 2000, **6**:1579-1589
53. Yamasaki L, Jacks T, Bronson R, Goillot E, Harlow E, Dyson NJ: **Tumor induction and tissue atrophy in mice lacking E2F1.** *Cell* 1996, **85**:537-548
54. Lillibridge CD, O'Connell BC: **In human salivary gland cells, overexpression of E2F1 overcomes an Interferon-γ – and Tumor Necrosis factor-α-induced growth arrest but does not result in complete mitosis.** *J Cell Physiol* 1997, **172**:343-350
55. Van de Craen M, Declercq W, Van den brande I, Fiers W, Vandenabeele P: **The proteolytic procaspase activation network: an in vitro analysis.** *Cell Death Differ* 1999, **6**:1117-24
56. Chu K, Niu X, Williams L: **A Fas-associated protein factor, FAF1, potentiates Fas-mediated apoptosis.** *Proc Natl Acad Sci (USA)* 1995, **92**:11894-11898
57. O'Dell W: **Fas signaling pathway.** *Biocarta* 2001 [www.biocarta.com/pathfiles/fasPathway.asp]
58. Tran SEF, Holmstrom TH, Ahonen M, Kahari V-M, Eriksson JE: **MAPK/ERK overrides the apoptotic signaling from Fas, TNF, and TRAIL receptors.** *J Biol Chem* 2001, **276**:16484-16490
59. Mikula M, Schreiber M, Husak Z, Kucerova L, Ruth J, Wieser R, Zatloukai K, Beug H, Wagner EF, Baccarini M: **Embryonic lethality and fetal liver apoptosis in mice lacking the c-raf-1 gene.** *EMBO J* 2001, **20**:1952-1962
60. Jaskoll T, Choy HA, Melnick M: **Glucocorticoids, TGF-beta, and embryonic mouse salivary gland morphogenesis.** *J Craniofac Genet Dev Biol* 1994, **14**:217-230
61. Torgerson TR, Colosia AD, Donahue JP, Lin Y-Z, Hawager J: **Regulation of NF-κB, AP-1, NFAT, and STAT 1 nuclear import in T Lymphocytes by noninvasive delivery of peptide carrying the nuclear localization sequence of NF-κB p50.** *J Immunol* 1998, **161**:6084-6092
62. Boothby M: **Specificity of SN50 for NF-κB?** *Nature Immunol* 2001, **2**:471
63. Das J, Chen C-H, Yang L, Cohn L, Ray P, Ray A: **A critical role for NF-κB in Gata3 expression and Th2 differentiation in allergic airway inflammation.** *Nature Immunol* 2001, **2**:45-50
64. Ray A: **Response.** *Nature Immun* 2001, **2**:471-472
65. Bains W: **The parts of life.** *Nature Biotech* 2001, **19**:401-402
66. Watts DJ, Strogatz SH: **Collective dynamics of 'small-world' networks.** *Nature* 1998, **393**:440-442
67. Asthagiri AR, Lauffenberger DA: **A computational study of feedback effects on signal dynamics in a mitogen-induced protein kinase (MAPK) pathway model.** *Biotechnol Prog* 2001, **17**:227-239
68. Theiler K: **The House Mouse.** *New York: Springer-Verlag* 1989
69. Specht D: **Probabilistic neural networks for classification, mapping, or associative memory.** *Proc IEEE Int Conf Neural Networks* 1988, **1**:525-532
70. Specht D: **Probabilistic neural networks.** *Neural Networks* 1990, **3**:109-118
71. Specht D, Shapiro P: **Generalization accuracy of probabilistic neural networks compared with back-propagation networks.** *Proc Int Joint Conf Neural Networks* 1991, **1**:887-892
72. Chen C: **Fuzzy logic and neural network handbook.** *New York: McGraw-Hill* 1996
73. Sokal RR, Rohlf FJ: **Biometry.** *New York: Freeman* 1981
74. Abe K, Saito H: **Neurotrophic effect of basic fibroblast growth factor is mediated by the p42/p44 mitogen-activated protein kinase cascade in cultured rat cortical neurons.** *Dev Brain Res* 2000, **122**:81-85
75. Callaerts P, Halder G, Gehring W: **PAX-6 in development and evolution.** *Annu Rev Neurosci* 1997, **20**:483-532
76. Candela M, Barker SC, Ballon LR: **Fibroblast growth factor increases TNF alpha-mediated prostaglandin E2 production and TNF alpha receptor expression in human fibroblasts.** *Mol Cell Biochem* 1993, **120**:43-50
77. Cano E, Mahadevan L: **Parallel signal processing among mammalian MAPKs.** *Science* 1995, **4**:117-122
78. Coppola D, Ferber A, Miura M, Sell C, D'Ambrosio C, Rubin R, Baserga R: **A functional insulin-like growth factor I receptor is required for the mitogenic and transforming activities of the epidermal growth factor receptor.** *Mol Cell Biol* 1994, **14**:4588-4595
79. Davis RJ: **Signal transduction by the JNK group of MAP kinases.** *Cell* 2000, **103**:239-252
80. De Benedetti F, Alonzi T, Moretta A, *et al*: **Interleukin 6 causes growth impairment in transgenic mice through a decrease in insulin-like growth factor-I: a model for stunted growth in children with chronic inflammation.** *J Clin Inv* 1997, **99**:643-650
81. de Martin R, Schmid J, Hofer-Warbinek R: **The NF-κB/Rel family of transcription factors in oncogenic transformation and apoptosis.** *Mutation Res* 1999, **437**:231-243
82. Glienke J, Fenten G, Seemann M, Sturz A, Thierauch K-H: **Human SPRY2 inhibits FGF2 signalling by a secreted factor.** *Mech Dev* 2000, **96**:91-99
83. Harris V, Coticchia C, Kagan B, Ahmad S, Wellstein A, Riegel A: **Induction of the angiogenic modulator fibroblast growth factor-binding protein by epidermal growth factor is mediated through both MEK/ERK and p38 signal transduction pathways.** *J Biol Chem* 2000, **275**:10802-10811
84. Hart K, Robertson S, Kanemitsu M, Meyer A, Tynan J, Donoghue D: **Transformation and stat activation by derivatives of FGFR1, FGFR3, and FGFR4.** *Oncogene* 2000, **19**:3309-3320
85. Janknecht R, Hunter T: **Nuclear fusion of signaling pathways.** *Science* 1999, **284**:443-444
86. Janson W, Brandner G, Siegel J: **Butyrate modules DNA-damage-induced p53 response by induction of p53-independent differentiation and apoptosis.** *Oncogene* 1997, **15**:1395-1406
87. Kelliher M, Grimm S, Ishida Y, Kuo F, Stanger B, Leder P: **The death domain kinase RIP mediates the TNF-induced NF-κB signal.** *Immunity* 1998, **8**:297-303
88. Klint P, Kanda S, Kloog Y, Claesson-Welsh L: **Contribution of Src and Ras pathways in FGF-2 induced endothelial cell differentiation.** *Oncogene* 1999, **18**:3354-3364
89. Kyriakis J, Banerjee P, Nikolakaki E, *et al*: **The stress-activated protein kinase subfamily of c-Jun kinases.** *Nature* 1994, **369**:156-160
90. Li F, Ambrosini G, Chu E, Plescia J, Tognin S, Marchisio PC, Altieri DC: **Control of apoptosis and mitotic spindle checkpoint by survivin.** *Nature* 1998, **396**:580-583
91. Massague J, Blain S, Lo R: **TGF-β signaling in growth control, cancer, and heritable disorders.** *Cell* 2000, **103**:295-309
92. Minowada G, Jarvis L, Chi C, Neubuser A, Sun X, Hacohen N, Krasnow MA, Martin GR: **Vertebrate sprouty genes are induced by FGF signaling and can cause chondrodysplasia when overexpressed.** *Development* 1999, **126**:4465-4475
93. Prisco M, Hongo A, Giulia R, Sacchi A, Baserga R: **The insulin-like growth factor I receptor as a physiologically relevant target of p53 in apoptosis caused by interleukin-3 withdrawal.** *Mol Cell Biol* 19971084-1092
94. Qu Z, Huang X, Stenberg P, Le A-C, Planck S, Rosenbaum J: **Synthesis of basic fibroblast growth factor by murine mast cells.** *Int Arch Allergy Immunol* 1998, **115**:47-54
95. Richardson N, Chamberlain C, McAvoy J: **IGF-I enhancement of FGF-induced lens fiber differentiation in rats of different ages.** *Inv Ophtal Vis Sci* 1993, **34**:3303-3312
96. Ring C, Cho K: **Insights from model systems specificity in transforming growth factor-beta signaling pathways.** *Am J Hum Genet* 1999, **64**:691-697

97. Schlessinger J: **Cell Signaling by receptor tyrosine kinases.** *Cell* 2000, **103**:211-225
98. Shikama N, Lee C-W, France S, Delavaine L, Lyon J, Krstic-Demonacos M, La Thangue NB: **A novel cofactor for p300 that regulates the p53 response.** *Mol Cell* 1999, **4**:365-376
99. Sluss H, Barrett T, Derijard B, Davis R: **Signal transduction by tumor necrosis factor mediated by JNK protein kinases.** *Mol Cell Biol* 1994, **14**:8376-8384
100. Stroschein S, Wang W, Zhou S, Zhou Q, Luo K: **Negative feedback regulation of TGF-beta signaling by the SnoN oncoprotein.** *Science* 1999, **286**:771-774
101. Suzuki A, Ito T, Kawano H, *et al*: **Survivin initiates procaspase 3/p21 complex formation as a result of interaction with Cdk4 to resist Fas-mediated cell death.** *Oncogene* 2000, **19**:1346-1353
102. Szebenyi G, Fallon J: **Fibroblast growth factors as multifunctional signaling factors.** *Int Rev Cyt* 1999, **185**:45-106
103. Tan M, Wang Y, Guan K, Sun Y: **PTGF-beta, a type beta transforming growth factor (TGF-beta) superfamily member, is a p53 target gene that inhibits tumor cell growth via TGF-beta signaling pathway.** *Proc Natl Acad Sci (USA)* 2000, **97**:109-114
104. Tomoda K, Kubota Y, Kato J-Y: **Degradation of the cyclin-dependent-kinase inhibitor p27kip1 is instigated by Jab 1.** *Nature* 1999, **398**:160-165
105. Ulloa L, Doody J, Massague J: **Inhibition of transforming growth factor-beta/SMAD signalling by the interferon-y/STAT pathway.** *Nature* 1999, **397**:710-713
106. Visser J, Themmen A: **Downstream factors in transforming growth factor-beta family signaling.** *Mol Cell End* 1998, **146**:7-17
107. Warburton D, Schwarz M, Tefft D, Flores-Delgado G, Anderson K, Cardoso W: **The molecular basis of lung morphogenesis.** *Mech Dev* 2000, **92**:55-81
108. Wu Y, Tewari M, Cui S, Rubin R: **Activation of the insulin-like growth factor-I receptor inhibits tumor necrosis factor-induced cell death.** *J Cell Phys* 1996, **168**:499-509